Available online at www.sciencedirect.com

ScienceDirect

Energy Procedia 69 (2015) 1277 – 1286

Energy Procedia

International Conference on Concentrating Solar Power and Chemical Energy Systems
SolarPACES 2014

Enhancing the profitability of solar tower power plants through thermoeconomic analysis based on multi-objective optimization

R. Guédez[a]*, M. Topel[a], J. Spelling[b] and B. Laumert[a]

[a] *Department of Energy Technology, KTH Royal Institute of Technology, 100 44, Stockholm, Sweden*
[b] *High Temperature Processes Unit, IMDEA Energy Institute, 28935 Móstoles, Spain*

Abstract

Solar tower power plants with integrated thermal energy storage units represent one of the most promising technologies for enhancing the economic viability of concentrating solar power in the short term. Tower systems allow higher concentration ratios to be achieved, which in turn means higher fluid operating temperatures and thus higher power cycle efficiencies. Moreover, the integration of storage allows power production to be shifted from times where there is low demand to periods where electricity prices are higher, potentially enhancing the profitability of the plant despite representing an additional upfront cost. The variable nature of the solar resource and the myriad potential roles that storage can assume, together with the complexity of enhancing the synergies between the three blocks: the solar field, the storage block and power block, make the design of these power plants a challenging process. This paper introduces a comprehensive methodology for designing solar tower power plants based on a thermoeconomic approach that allows the true optimum trade-off curves between cost, profitability and investment to be identified while simultaneously considering several operating strategies as well as varying critical design parameters in each of the aforementioned blocks. The methodology is presented by means of analyzing the design of a power plant for the region of Seville. For this location, results show that similar profits, measured in terms of the internal rate of return, can be achieved from different power plant configurations in terms of sizing and operating strategy, each associated to different investments. In particular, optimum configurations found corresponded to larger power blocks with medium-to-large solar field and storage blocks that allow the plants to operate continuously throughout the day and be shut down during midnight. Moreover, it is shown that for a fixed power block size it can also be economically interesting to consider smaller storage units and adopt instead a peaking strategy, as this can still be profitable whilst representing a lower investment, thus lower risk.

Peer review by the scientific conference committee of SolarPACES 2014 under responsibility of PSE AG

* Corresponding author. Tel.: +46-(0)-8-790-8643
E-mail address: rafael.guedez@energy.kth.se

Peer review by the scientific conference committee of SolarPACES 2014 under responsibility of PSE AG
doi:10.1016/j.egypro.2015.03.155

Keywords: multi-objective optimization, concentrating solar power, techno-economic analysis, thermal energy storage

1. Introduction

Despite continued efforts from academia, industry and policy makers, the development of new concentrating solar power (CSP) plants is threatened by the relatively high costs of this technology, which is not yet competitive with other means of power generation, including other renewables such as solar photovoltaics and wind [1]. The ability to integrate thermal energy storage (TES) has been acknowledged as one of the key means to enhance the economic viability of CSP plants either by increasing the capacity factor or by allowing the solar input to be decoupled from the electrical output energy and thereby generate electricity during peak hours when revenues are highest [2][3]. However, the integration of TES units also increases the capital expenditures (CAPEX) of the power plant, increasing the risk associated to the project. As such, the choice of TES size and operating strategy becomes a critical design parameter from the early stages of the design process, and this choice will be strongly influenced not only by the level of profitability that can be achieved but also by the CAPEX that investors are willing to finance. Previous work by the authors has shown that for a specific operating strategy, whether peaking or continuous-dispatch, it is possible to identify optimum TES sizes yielding the lowest levelized cost of electricity (LCOE), along with the required solar field (SF) investment for each TES size [4][5]. However, such studies have been based on fixed power block (PB) designs, whereas in reality turbine specifications and steam cycle thermodynamics can influence on the final choice of TES size. Selection of the economically optimal PB design will also depend on the operating strategy, as both cycle size and specifications have a great impact on both CAPEX and operational expenditures (OPEX) of the power plant. As such, the objective of the present work is to introduce a comprehensive methodology for identifying the true optimum trade-off curves between cost, profitability and investment for solar tower power plants (STPPs) by simultaneously considering TES integration strategies together with SF and PB design. By identifying such curves, a wide range of optimum designs can be presented to investment decision makers, who can then choose a configuration that best satisfies their needs in terms of investment and profits.

Nomenclature

α	Capital return factor
BOP	Balance of Plant
C	Costs
CAPEX	Capital Expenditures
CSP	Concentrating Solar Power
E_{net}	Electricity Produced
EPC	Engineering, Procurement and Construction
EOH	Equivalent Operating Hours
HTF	Heat Transfer Fluid
i	Real interest rate
IRR	Internal Rate of Return
k_{ins}	Insurance rate
LCOE	Levelized Cost of Electricity
OM	Operating Mode
OPEX	Operational Expenditures
PB	Power Block
rec	Receiver
SF	Solar Field
SM	Solar Multiple
STPP	Solar Tower Power Plant
TES	Thermal Energy Storage
TTD	Terminal Temperature Difference

2. Solar tower power plants

The typical layout of a STPP with integrated TES is shown in Fig. 1, where two thermodynamic cycles can be distinguished: the heat transfer fluid (HTF) cycle (depicted in thick black lines) and the steam cycle. At nominal conditions, the cold molten salts are initially stored in a tank (CT) and are pumped-up to the receiver (R) mounted in the top of the solar tower, where energy is provided by the surrounding heliostat mirrors that compose the SF. Once heated, the molten salts are stored in the hot tank (HT) which is discharged at a specified flow rate to enter the steam generation train, comprised of the economizer, the evaporator, the superheater and the reheater, respectively denoted as EC, EV, SH and RH in Fig. 1. Lastly, the figure shows that the steam PB corresponds to a typical reheat Rankine cycle with extractions for feedwater preheating. In this steam PB, the high pressure and low pressure turbines, the deaerator and the air cooled condenser are denoted as HP-ST, LP-ST, D and ACC respectively.

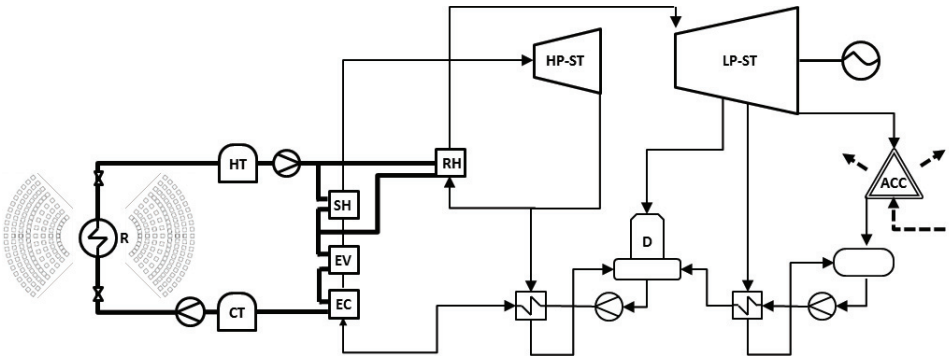

Fig. 1. Layout of the STPP with TES

The layout of the STPP with TES grants great flexibility concerning the operation of the plant. In this regard, and as mentioned in §1, depending on the targeted market roles TES system can be designed in different ways. If continuous power production is desired, for example to provide baseload power, a large TES unit can be combined with a large SF and a relatively smaller PB. In this way, all the daytime heat input from the Sun can be collected and stored. With a turbine size smaller than the nominal solar heat input during peak hours, TES allows the collected energy to be spread over the whole 24 hours of the day, for continuous power production. Another option is to store heat and shift load to peak demand hours, so that instead of attempting to produce electricity continuously, TES allows to shift power production to times when it is needed more and thus sell it for higher prices. An example would be to store energy in the morning and use it to extend power production into the evening when production from other sources such as photovoltaic decreases. Furthermore, in markets where the prices are known to be higher in the evenings or with a pronounced peak demand time, TES allows shifting production to such hours so as to assure achieving maximum revenues. Regardless the operating strategy: continuous-dispatch or peaking, Table 1 shows the different plant operating modes (OMs) that can be identified in a STPP with TES.

Table 1: Operating Modes of the STPP with TES

OMs	Description
OM1	The STPP is online. The TES hot tank is being charged by heat from the SF whilst simultaneously being discharged at a flow rate that meets nominal power output.
OM2	There is no heat input from the SF but there is enough energy stored in the TES hot tank to allow the STPP operate at its nameplate capacity (e.g. either to extend production or for use during specified peaking hours).
OM3	The TES hot tank is being charged with heat input from the SF but the STPP is offline (e.g. energy is stored for peak hours)
OM4	The STTP is offline as there is neither enough energy from the SF nor stored in the TES hot tank.

3. Thermo-economic modeling approach

The analysis of the STPP with TES was performed using DYESOPT (standing for Dynamic Energy Systems Optimizer), a thermoeconomic modeling tool developed by the authors, which requires location-specific inputs (such as economic indicators, hourly meteorological conditions and electricity pool prices) as well as power plant design specifications and cost functions at the component level. These inputs allow the design of the power plant at nominal conditions, afterwards used for annual performance simulation using TRNSYS which results are finally used for thermoeconomic performance evaluation. Fig. 2 schematizes a simplified version of the flow of information and calculations in the tool, where the required input data is differentiated by colors depending on the nature of the data: design configuration related (dark grey), location-related (grey) and cost functions (white). The following sub-sections aim at briefly providing an insight to each of the blocks shown: the required input data, each of the processes and calculations performed, and the outputs obtained from the tool.

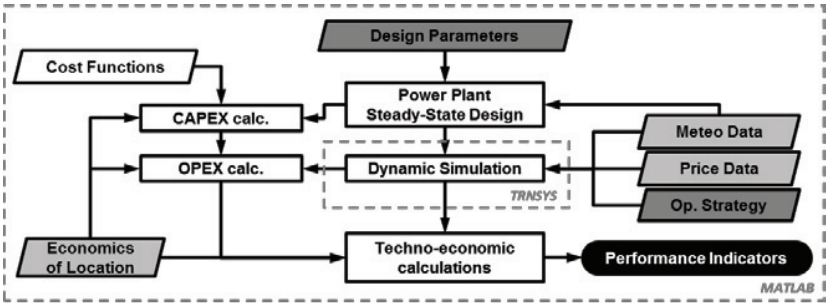

Fig. 2. Simplified schematics of information flow in DYESOPT

3.1. Input data: variable design parameters and location-related information

As described in §2, three main blocks can be identified in the typical STPP layout: the SF, the TES-HTF cycle and the steam PB. Within each of these blocks there exist critical design parameters that can strongly impact the overall performance of the power plant. Table 2 displays the most relevant parameters that must be input for designing the SF and TES-HTF blocks in order to estimate the STPP performance. Similarly, Table 3 shows the critical inputs corresponding to the steam PB. In both tables, the critical parameters are shown together with the limit values within which they can vary. From these values, the optimizer can evaluate all possible combinations and thus find the optimal designs as it is explained in §3.5. All other design parameters, that were chosen not to be shown here, were assumed to have fixed values with data corresponding to conventional STPPs [6].

Table 2: Critical input design parameters for SF and TES-HTF Cycle

Solar Field			Thermal Energy Storage – HTF Cycle		
Solar Multiple	0.5 : 3	[-]	TES Capacity	1 : 18	[h]
Tower Height	80 : 250	[m]	TES tank height	10 : 20	[m]
Heliostat Mirror Area	60 : 140	[m^2]	TES dispatch strategy	peaking or continuous-dispatch	
Receiver Diameter	10 : 30	[m]	Control variable δ_1	5 : 15	[%]
Receiver Height	10 : 30	[m]	Control variable δ_2	70 : 90	[%]
Heliostat reflectivity	94	[%]	Dry loss Coefficient	0.01	[W/m^2]
Nominal Receiver Efficiency	88	[%]	Wet loss Coefficient	0.01	[W/m^2]
Maximum Receiver Temperature	565	[C]	Salt Pumps Efficiency	85	[%]

Table 3: Critical input design parameters for PB – Steam Cycle

Power Block – Steam Cycle					
Net Power Output	15 : 180	[MW_e]	Superheater Pinch	10 : 14	[C]
Nominal Condensing Split	16 : 26	[C]	Economizer Pinch	8 : 12	[C]
Inlet HP-ST pressure	75 : 170	[bar]	Reheater TTD	10 : 16	[C]
Inlet LP-ST pressure	10 : 75	[bar]	Feedwater Preheaters TTD	2 : 4	[C]
Number of HP-ST extractions	0 : 3	[-]	Pump Efficiencies	85	[%]
Number of LP-ST extractions	0 : 3	[-]	Generator Efficiency	95	[%]

In this study, the Spanish electricity market is considered, as it is the only market to date with an operational molten salt STPP with TES [6]. In particular, for a chosen location near Seville, Spain, a whole year's worth of price and meteorological data were gathered. The meteorological data used corresponds to typical weather data for the location at coordinates 37°34'N, 2°39'E with a time span of ten minutes as extracted from the HelioClim-3 dataset [7] (with an average DNI of 2100 kWh/m^2/yr), whereas the Spanish hourly price data was obtained from the market operator for the year 2012 [8] (with mean and maximum prices of 80 and 180 USD/MWh respectively).

3.2. Steady-state design and dynamic modeling of the STPP

The first process in DYESOPT corresponds to the design of the power plant at nominal conditions (steady state), based on the input data described in §3.1. For such purpose, individual steady state models for each of the components existing in the power plant were implemented. The equations governing these models were extracted from [9] (as gathered from [10][11][12]) for the SF, from [13] for the HTF cycle and from [14][15] for the PB. The nominal design allows for sizing each of the components in the power plant, information needed for the dynamic modeling. In this regard, each of the blocks in the STPP: the SF, the TES-HTF cycle and the PB, has been modeled in detail in the TRNSYS simulation studio [16]. Within TRNSYS, the solar collector field was modeled using STEC Types 394 and 395 for the heliostat field and central receiver respectively [17]. TRNSYS Type 394 uses an externally supplied efficiency matrix which maps the solar position to a value of overall heliostat field efficiency. This matrix is determined using an in-house model, described in a previous work [9]. The TRNSYS Type 39 variable volume tank [16] was used to model both the hot and cold tanks of the two-tank direct TES system, with additional HTF fluid properties data obtained from [13]. Concerning the PB, the transient model calculates the steam mass flow input to the turbine based on the conditions of the hot molten salts at the inlet to the steam-generator heat exchanger train, using components from the TRNSYS STEC and Heat Exchangers libraries, as described in [16][17]. All of these components have been validated in previous studies for the transient modeling of Rankine cycles for CSP plants [18]. Off-design performance of the power block takes into account variations in efficiency and mass flows as a function of the turbine inlet conditions using the Stodola ellipse law [19].

In order to best emulate the dynamic behavior of the STPPs, logical control variables are set in TRNSYS. Fig. 3 describes the reasoning behind the control strategies for both: continuous-dispatch and peaking operating strategies.

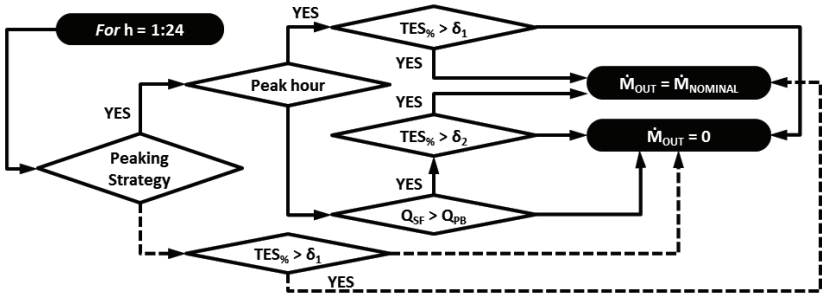

Fig. 3 TES dispatch control strategy in STPP

It can be seen that in case a continuous-dispatch strategy is desired (dashed lines) the model is set to run at nominal capacity whenever the level of the hot tank exceeds a user-specified minimum level, δ_1. Alternatively, in case of a peaking strategy, a prior subroutine defines which hours of the day are to be considered peaking hours depending on the input TES capacity, the expected radiation and the price curves. Then for every hour, the model checks if it is in presence of a peaking hour. In case of a peaking hour, the hot tank is dispatched at nominal capacity whenever its level is higher than δ_1. If instead the hour is not a peaking hour, but there is still energy from the SF and the hot tank level is higher than a user-specified minimum allowable level for dispatching whilst charging, δ_2, the plant operates at its nameplate capacity as well. Under any other circumstances, the plant is set to be offline.

3.3. Cost functions and economic performance indicators

In order to measure the economic performance of the STPP, two main performance indicators were considered, namely the LCOE and the internal rate of return (IRR), both of them function of CAPEX and the annual OPEX. CAPEX was calculated by use of Eq. 1, as the sum of all direct and indirect investment costs. Direct costs consider all equipment related costs from purchasing, to installation on site, whereas indirect costs relate to costs undertaken during the commissioning process such as land purchase, taxes and labor (both engineering and management). These costs were estimated based on the models described in [20][21]. These models use reliability functions for cost scaling-up based on cost values from reference plants and respective material and labor cost multipliers for ensuring that results are sensitive to specific locations. In this study, reference cost values for Spain were extracted from [22]. A typical reliability function for cost scaling-up is shown in Eq. 2, where the cost of equipment *'m'*, can be calculated based on n_1 reference cost values C_{ref}, which are sensitive to n_2 critical design parameters *'X'*, each in different degrees of relevance expressed by n_2 size scaling exponents '*y*'.

$$CAPEX = \left\{ + \begin{array}{c} C_{direct} \\ C_{indirect} \end{array} \right\} = \left\{ + \begin{array}{c} C_{PB} + C_{SF} + C_{TES} + C_{rec} + C_{tower} + C_{BOP} + C_{site} + C_{contingencies} \\ C_{EPC\_ownership} + C_{TAX} + C_{land} \end{array} \right\} \quad (1)$$

$$C_m = \sum_{\gamma=1}^{n_1} \left\{ C_{ref,\gamma} \cdot \prod_{\beta=1}^{n_2} \left[\left(\frac{X_{m,\beta}}{X_{ref,\beta}} \right)^{y_\beta} \right] \right\} \quad (2)$$

Annual OPEX was calculated by means of Eq. 3, as a function of the annual burdened labor costs, costs for contracted services, utility bills and other variable miscellaneous costs related to material requirements and equipment maintenance. Similarly to CAPEX, annual OPEX costs were estimated based on the model described in [20] and using reference cost values from [22].

$$OPEX = C_{labor} + C_{contract\_services} + C_{utilities} + C_{miscellaneous} \quad (3)$$

The LCOE was calculated using Eq. 4, as a function of the CAPEX, the annual OPEX and the total electricity produced throughout the year E_{net}. The capital return factor α was calculated using Eq. 5, where *i* stands for the real interest rate, *n* for the plant lifetime and k_{ins} for the insurance rate, with values extracted from [23], as used in [4].

$$LCOE = \left[\alpha \cdot CAPEX + OPEX \right] \cdot \left(E_{net} \right)^{-1} \quad (4)$$

$$\alpha = \left[i \cdot (1+i)^n \right] \cdot \left[(1+i)^n - 1 \right]^{-1} + k_{ins} \quad (5)$$

Lastly, the IRR is calculated by means of Eq. 6 as the discount rate that makes the net present value (NPV) of all cash flows equal to zero at the end of the lifetime of the SSTCC. In addition to the aforementioned parameters used to calculate the LCOE, Eq. 6 is also a function of the years of plant construction n_{con}, the years of plant operation n_{op}, the annual revenue from electricity sells λ_{el}, the years of plant decommissioning n_{dec} and the decommissioning costs C_{dec}, based on cost models [20][21] and hourly price data [8], together with commissioning values from [9].

$$NPV = -\sum_{t=0}^{n_{con}-1} \frac{CAPEX}{n_{con}(1+IRR)^t} + \sum_{t=n_{con}}^{n_{con}+n_{op}-1} \frac{\lambda_{el} - OPEX}{(1+IRR)^t} - \sum_{t=n_{con}+n_{op}}^{n_{con}+n_{op}+n_{dec}-1} \frac{C_{dec}}{n_{dec}(1+IRR)^t} = 0 \quad (6)$$

3.4. Multi-objective optimization analysis in DYESOPT

As described in §3.3, the performance of the STPP can be measured by means of several performance indicators. In this way, multiple design objectives can be identified and these, for instance, are often conflicting between them, such as maximizing the IRR (or minimizing LCOE) whilst simultaneously minimizing CAPEX or OPEX. As such, no single optimum can be found meeting all objectives, but instead it is possible to find the maximum IRR for a specific CAPEX, thus yielding a trade-off of multiple optimal designs best comprising investment and profitability of the projects. The analysis of these trade-off curves enables to have a range of solutions that can be presented to investment decision makers, who can then choose the desired compromise between the objectives. In order to examine the trade-offs, DYESOPT incorporates a modified version of QMOO, a multi-objective optimizer set to estimate Pareto-optimal fronts from a population-based evolutionary algorithm developed at the Industrial Energy Systems Laboratory in Lausanne [24]. Fig. 4 shows the scheme of the information flow in DYESOPT when running an optimization study. Unlike Fig. 2, in this case, the first requirement from the users perspective is to set the conflicting objectives and then specify a range of values within which the design parameters described in §3.1 can vary. Next, by varying such inputs the optimizer performs as many simulations as needed until clear Pareto fronts can be distinguished, in which case the convergence is reached and results are both stored and displayed graphically.

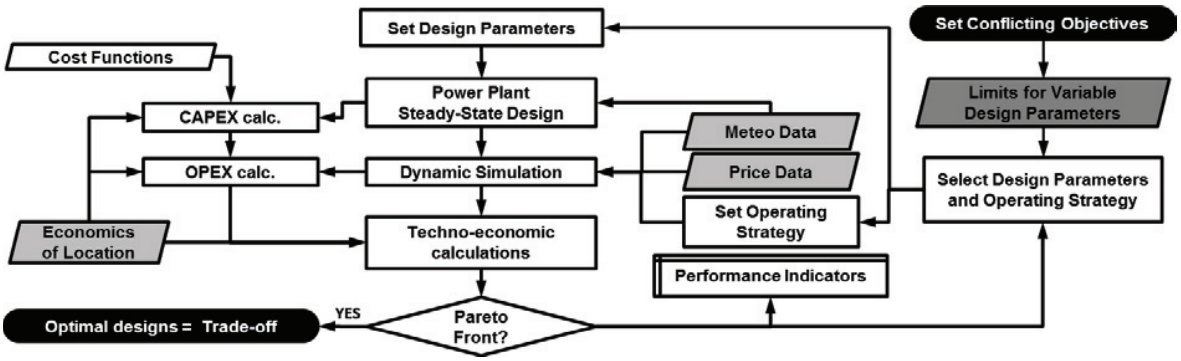

Fig. 4 Schematics of information flow in DYESOPT for Multi-Objective Optimization Analysis

4. Results from thermoeconomic modeling of the STPP

The results from evaluating the design of a STPP for a location in Seville are shown in Fig. 5. The trade-offs shown are yielded when the methodology described in §3 is followed and all critical parameters can vary within the respective limits specified in Table 2 and Table 3. In this way, for all the plots, each point represents a specific plant configuration resulting from the particular combination of inputs chosen by the optimizer. In all four plots displayed, the same trade-off between maximizing IRR and minimizing the CAPEX is shown. In general, it can be seen that a higher profitability margin can be reached when the upfront investment is higher. However, it is shown that above a certain CAPEX (approx. 800 million USD) an increase in the IRR of approximately 0.5% (absolute) will imply investing 1.5 times more money, thus representing a higher risk project and potentially less interesting for investors.

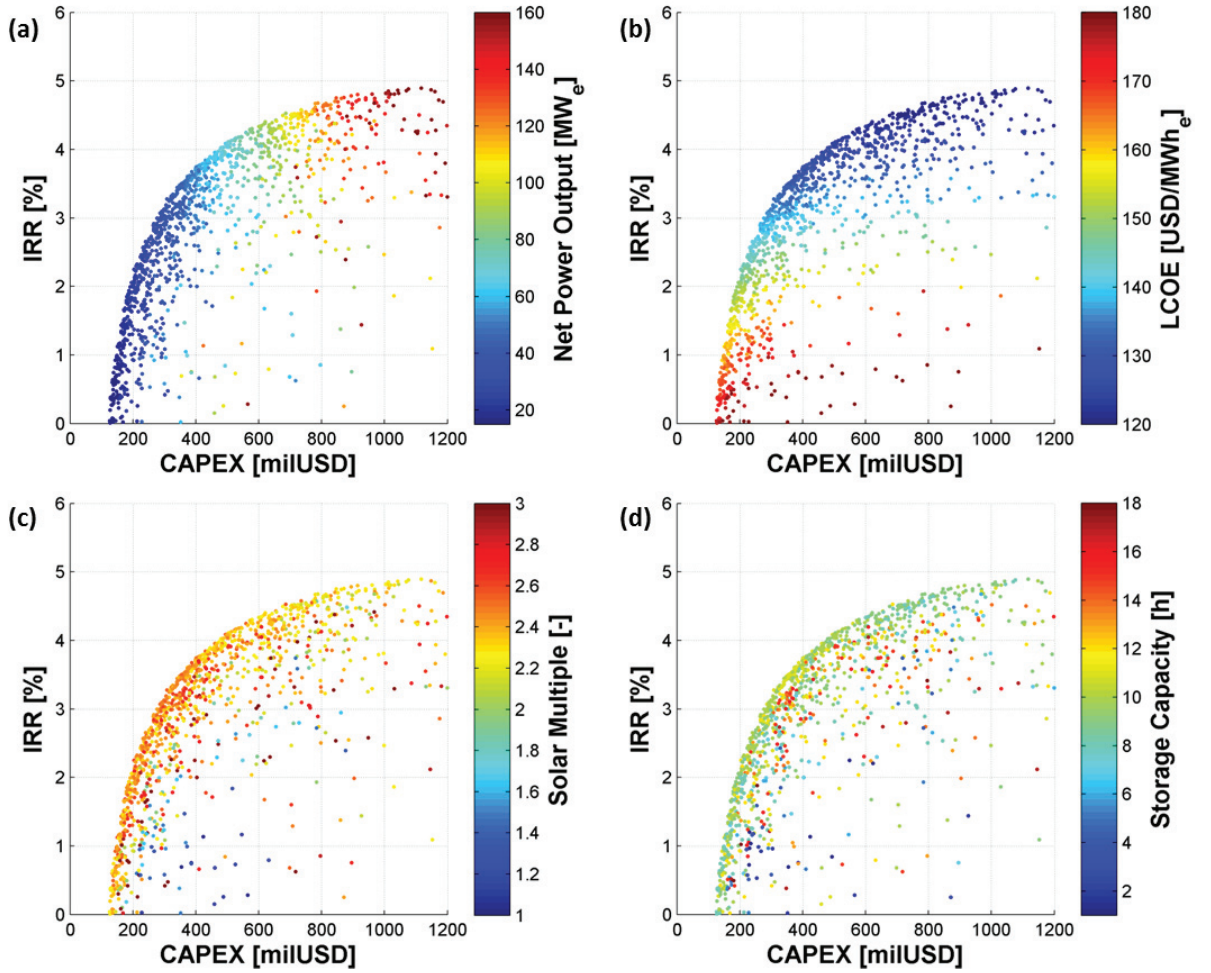

Fig. 5 Trade-off between IRR and CAPEX when varying all critical design parameters

Additionally, Fig. 5 shows how critical sizing parameters influence on the evaluation of the optimal trade-off. From (a), (c) and (d) it can be concluded that for this location larger PBs, linked to higher CAPEX, can guarantee higher IRR values when coupled with SFs with SM values varying between 2.2 and 2.6 and a TES system of approximately 8 to 11 hours. Moreover, (c) and (d) show that the optimal SF-TES size combination was found to be similar regardless the size of the PB. These results were expected as for this location in particular, night peak prices are not considerably higher than the daily average [8] partly due to the excess of installed capacity [24], which leads the optimizer to suggest STPP configurations able to operate continuously during the critical consumption hours (morning, afternoon and night) but that are shutdown during midnight. In any case, optimal IRR values were found to be relatively low and thus implying that projects would not represent an economically interesting enough option for investors, reaffirming the current trend for CSP in Spain [22]. Lastly, it can be seen from (b) that setting the optimizer for minimizing the LCOE values instead of maximizing the IRR, would have yielded a similar optimal front, with the trend of being able to reach lower LCOE values as the CAPEX is increased.

Alternatively, Fig. 6 shows the results from the optimizer for a fixed 110 MWe (net) STTP. The optimal trade-off curve between IRR and CAPEX and its relation with the operating strategy is displayed in (a). Moreover, (c) shows the relation between SM and TES size with regards of optimal designs. From these two plots, it can be seen that STPP with smaller TES (5-6 hours) can also yield ‘high’ IRR values (4%) at a lower risk if these are operated as ‘peaker’ plants; (c) also shows that, for each case, a relation between optimal SF and TES size can be identified.

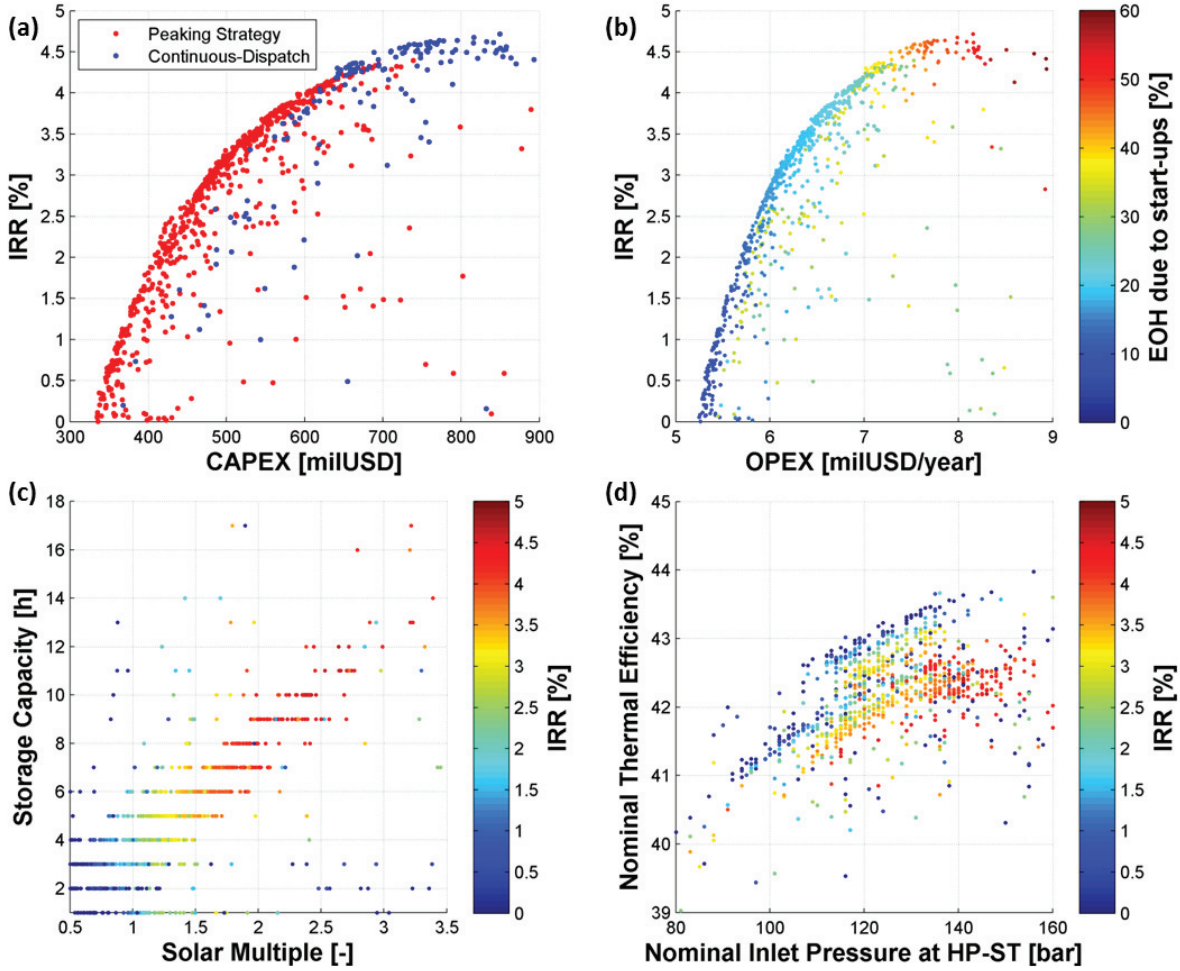

Fig. 6 Optimizer results for a 100 MW_e (net) STPP when varying all other critical design parameters

Fig. 6 (b) shows the relation between the annual OPEX and the IRR and relates it with the fraction of equivalent operating hours that occur due to start-ups (EOHs), based on the theory described in [5]. By comparing with (a), it can be seen that by adopting a peaking strategy, despite incurring in increasing the number of start-ups, the fraction of EOHs is reduced as most of these start-ups occur during typical hot start conditions. This, in general, is beneficial for the lifetime of the turbine and implies that most of its maintenance requirements are due to normal operating conditions rather than from the cycling behaviour of the STPP. Lastly, (d) shows the relation between the nominal live steam operating pressure and the efficiency of the PB and relates it to the IRR. From this plot, it can be seen that, in general, designing for achieving the highest thermal efficiencies will not always yield the most profitable design, as the highest IRR values were found not for the highest efficiencies but for less (42% instead of 44%).

5. Conclusions

A comprehensive methodology based on thermoeconomic analysis has been introduced to evaluate the design of CSP plants. The methodology couples technical design specifications together with meteorological and market price data and user-specified cost functions for estimating the economic performance of the plants, measured in terms of the CAPEX, the IRR and the LCOE. Moreover, it allows the user to identify trade-off curves containing optimal plant configurations that best comprise the profitability and investment of the projects by means of Pareto-optimality

analysis resulting from multi-objective optimization. In particular, the study describes the design process of a STPP for the region of Seville, Spain. For this case, the results show that when the power output is considered as a design variable, the highest IRR can be reached by plant configurations formed by large PBs (over 100 MWe), with medium-to-large TES systems (between 8 and 12 hours). However, it was found that not even optimised designs seem to be economically attractive for this location. Furthermore, for the case of a fixed PB net output of 110 MWe, discretized trade-offs plots as a function of the input critical design variables are shown to be useful for understanding the influence that each parameter has on the overall performance. In addition, it is shown how designs with completely different configurations and operating strategies can yield similar profit levels. Specifically, it is shown that although the highest profits are reached for larger PBs operating continuously, it is possible to achieve similar IRR at a lower risk (lower CAPEX) when developing projects with smaller SF and TES units but following a suitable peaking strategy. Finally, it can be generally stated that the methodology introduced in this work represents a useful approach for assessing the design of CSP plants and especially for assisting the decision making process at early stages of the design process.

Acknowledgements

This research has been funded by the TESCONSOL consortium, a KIC Innoenergy project, whose support is acknowledged. Special thanks are dedicated to Total S.A and Gas Natural Fenosa for their contribution to the development of the tool. Thanks are also given to the Industrial Energy Systems Lab at EPFL for the use of QMOO.

References

[1] International Renewable Energy Agency. “Concentrating Solar Power, Renewable Energy Technologies: Cost Analysis Series”, Volume I: Power Sector, IRENA Secretariat, Abu Dhabi, 2012
[2] C. Philibert, P. Frankl, Z. Dobrotkova. “Concentrating Solar Power: Technology Roadmap”, International Energy Agency, Paris, 2010
[3] P. Denholm, et al. “The value of energy storage for grid applications”, Technical Report NREL, TP-6A20-58465, Golden, 2013.
[4] R. Guédez et al. “Optimization of Thermal Energy Storage Integration Strategies for Peak Power Production by Concentrating Solar Power Plants”. Proceedings of the International SolarPACES Conference, Las Vegas, 2013.
[5] R. Guédez et al. “Reducing the number of turbine starts in concentrating solar power plant through the integration of thermal energy storage”. Proceedings of ASME TURBO EXPO, San Antonio, 2013
[6] Burgaleta J., Arias S., Ramírez D. “GEMASOLAR, The first tower thermosolar commercial plant with molten salt storage”. Proceedings of the International SolarPACES Conference, Marrakech, 2012.
[7] SoDa Solar Radiation Data, “Time Series of Solar Radiation Data”, retrieved from www.soda-is.com on March 2013.
[8] Operador del Mercado Ibérico de Energía, Polo Español S.A. (OMIE), “Annual Report from Market Results 2012”, OMIE, Madrid, 2013.
[9] J. Spelling. Hybrid Solar Gas Turbine Power Plants – A Thermoeconomic Analysis. Doctoral Thesis. KTH; Stockholm, 2013.
[10] B. Kistler, A User’s Manual for DELSOL3, Sandia National Laboratories, 1986.
[11] F. Collado, Quick Evaluation of the Annual Heliostat Field Efficiency, Solar Energy, Volume 82, pp. 379 – 384, 2008.
[12] Duffie J., Beckmann W., Solar Engineering of Thermal Processes, 3rd Edition, John Wiley & Sons, New Jersey, 2006.
[13] P. Gilman, N. Blair, M. Mehos et al. “Solar advisor model user guide for version 2.0”, Tech. Report NREL/TP-670-43704, Golden, 2008.
[14] Incropera F., DeWitt D., Bergman T. et al., Fundamentals of Heat and Mass Transfer, 6th Edition, John Wiley & Sons, New York, 2007.
[15] F. Staine, “Intégration énergetique des procedes industriels par la method du pincement etendue aux facteurs exergetiques”, PhD Thesis #1318, Swiss Federal Technology Institute, Lausanne, 1995.
[16] Solar Energy Laboratory at UW-M, “TRNSYS 16 a Transient System Simulation program”, Program Manual, Madison, 2007.
[17] P. Schwarzbözl, “STEC: A TRNSYS Model Library for Solar Thermal Electric Components”, 2006.
[18] S. Jones, R. Pitz-Paal, P. Schwarzbözl et al., “TRNSYS Modeling of the SEGS VI Parabolic Trough Solar Electric Generating System”, Proceedings of the Solar Forum, Washington DC, 2001.
[19] D. Cooke, “Modeling of Off-Design Turbine Pressures by Stodola’s Ellipse”, Energy Incorporated, Richmond, 1983.
[20] C. Turchi, G. Heath. “Molten Salt Power Tower Cost Model for the System Advisor Model”, Report, NREL/TP-5500-57625, Golden, 2013.
[21] WorleyParsons Group, “CSP Parabolic Trough Plant Cost Assessment”, Tech. Report NREL-0-LS-019-0001, Golden 2009.
[22] CSP Today. “CSP Solar Tower Report 2014: Cost, Performance and Thermal Storage”, Technical Report, FC Business Intelligence, 2013.
[23] A. Kerney, ESTELA, ProtermoSolar. “Solar Thermal Electricity 2025: Clean Electricity on demand: attractive STE cost stabilize energy production” Roadmap report, Dusseldorf, 2010.
[24] G. Leyland, “Multi-Objective Optimisation applied to Industrial Energy Problems”, PhD Thesis, EPFL, Lausanne, 2002.
[25] Red Eléctrica de España, “El Sistema Eléctrico Español: 2013”, Technical Report, Red Eléctrica de España, Madrid, 2014.